

---

# NEW COEVOLUTION DYNAMIC AS AN OPTIMIZATION STRATEGY IN GROUP PROBLEM SOLVING

---

A PREPRINT

**Francis F. Franco**

Department of Physics

Federal University of Jataí (UFJ)

Jataí, GO, Brazil, 75801-615

[francis.franco@educa.go.gov.br](mailto:francis.franco@educa.go.gov.br)

**Paulo F. Gomes**

Department of Physics

Federal University of Jataí (UFJ)

Jataí, GO, Brazil, 75801-615

[paulofreitasgomes@ufj.edu.br](mailto:paulofreitasgomes@ufj.edu.br)

October 28, 2024

## ABSTRACT

Coevolution on social models couples the time evolution of the network with the time evolution of the states of the agents. This paper presents a new coevolution dynamic allowing more than one rewiring on the network. We explore how this coevolution can be employed as an optimization strategy for problem-solving capability of task-forces. We used an agent-based model study how this new coevolution dynamic can help a group of agents whose task is to find the global maxima of NK fitness landscapes. Each agent can replace more than one neighbors, and this quantity is a tunable parameter in the model. These rewirings is a way for the agent to obtain information from individuals that were not previously part of its neighborhood. Our results showed that this tunable coevolution can indeed produce gain on the computational cost under certain circumstances. At low average degree (using a random network to connect the agents) and on easy landscape, more rewirings return lower cost, helping the agents to find the global maximum faster. However, at larger average degree and difficult landscape, the effect is more complex. At medium size systems, the coevolution brings optimal results when 3 or 4 neighbors are replaced.

**Keywords** Coevolution, Group Problem Solving, NK model, Random Network

## 1 Introduction

In society, it is common to face problems that require collaboration with other people, from everyday challenges to complex tasks, such as group projects at work. In this context, the search for more effective problem-solving strategies becomes a topic of great interest.

Social interactions are inherently complex such that, in recent years, numerous models of social behavior have emerged to explore this intricacy [1, 2, 3] using the framework of Network Science [4]. The nodes of the network represent individuals (or agents) with states defined by the social model while the connections represent the interactions between different individuals. The states of the individuals evolve following the set of rules from the dynamic social model in study. The network itself can also have a time evolution: links can be destroyed or created.

Presently, a prominent aspect under exploration within dynamic social processes on complex networks is coevolution: the evolution of the agent states is coupled to the evolution of the network [5, 6, 7]. This coevolution has been studied in different social models [8, 9, 10, 11, 12, 13, 14] and Evolutionary Games Theory [15, 16]. The rationale behind this dynamics is that co-evolutionary, or adaptive, network models offer a more accurate portrayal of real world systems compared to static or evolving networks. Empirical networks display both network dynamics (the evolution of network topology) and node state dynamics. Therefore, coevolution can be conceptualized as two simultaneous processes – link rewiring and state dynamics – mutually influencing each other.

The central idea of coevolution in social dynamics is the agent uses the social information (states of the agents) of his influence neighborhood (set of neighbors) to remove one neighbor and add a new one. And then, considering this new influence neighborhood, his social state will evolve in time accordingly. This mechanism can make a difference in cooperative processes, where one studies the performance of a set of individuals solving a given task [17, 18, 19]. Each individual not only uses his influence network, but also changes it if he thinks one neighbor may not give a proper contribution to solve the problem. This is specially important in imitative learning, where one tries to learn from an expert's experience and behavior [20, 21].

How to modify the influence network is an important point to achieve success. Analyzing a group performance in problem-solving can be intricate. Initially, one might assume that a larger number of individuals working towards the same objective would expedite reaching a solution. However, interpersonal interactions (such as everyone engaging in discussion) can lead to suboptimal outcomes, deviating from the desired solution [22, 23].

In this work we study the effect of a coevolution mechanism on a cooperative process problem. To address this question, we use an agent-based model where the agents can perform individual trial-and-test searches to probe a fitness landscape (exploration) or imitate a model agent – the best performing agent in their influence neighborhood at the trial (exploitation). The coevolution mechanism gives a chance for the agent to change his influence neighborhood on the exploitation case. We consider a scenario where the agents are fixed at the nodes of a random network and can interact with each other if they are connected. In addition, before each interaction the agent has a chance to change  $L$  agents within his influence neighborhood. This set of rules creates a time-dependent and adaptive network.

This work is organized as follows: In Section 2.1 we present a brief discussion about the NK model, in section 2.2 we define the computational cost, in section 2.3 we define how the agents are updated, in section 2.4 we define the proposed coevolution mechanism and in section 2.6 we described the random network used to connect the agents. Section 3 is dedicated to present and discuss the results and section 4 is dedicated to our final considerations.

## 2 Model

### 2.1 NK Fitness Landscapes

The NK model was introduced by Kauffman and Levin as a fitness model for adaptive evolution processes such as walking in rugged landscapes [24, 25]. This model has been extensively used in different studies of cooperative process and imitative learning [26, 27, 28, 29, 30]. It is well suited for example for the imperfect version of the imitative learning process [31], when one agent copies only part of the solution from an expert.

The system is composed of  $M$  agents described by a binary string (or vector) of  $N$  bits  $\mathcal{X} = (x_1, x_2, \dots, x_N)$  with  $x_i \in \{0, 1\}$ . In total there are  $2^N$  different vectors  $\mathcal{X}$ . Each string has a fitness  $f(\mathcal{X})$ , limited in the interval  $0.0 < f(\mathcal{X}) < 1.0$ , calculated as [32]:

$$f(\mathcal{X}) = \frac{1}{N} \sum_{i=1}^N \Phi_i(K, \mathcal{X}), \quad (1)$$

where  $\Phi_i(\mathcal{X})$  is the contribution of component  $i$  to the fitness of string  $\mathcal{X}$ . It depends on the state  $x_i$  as well as on the states of the  $K$  right neighbors of  $i$ , i.e.,

$$\Phi_i(K, \mathcal{X}) = \Phi_i(x_i, x_{i+1}, x_{i+2}, \dots, x_{i+K}), \quad (2)$$

with the arithmetic in the subscripts done modulo  $N$  [33]. The functions  $\Phi_i$  are  $N$  distinct real-valued functions on  $\{0, 1\}^{K+1}$ . As usually done, we assign to each  $\Phi_i$  a uniformly distributed random number in the unit interval, so that  $f(\mathcal{X}) \in (0, 1)$  [34].

The function  $f(\mathcal{X})$  has a global maximum  $f(\mathcal{X}_M) = F$  at the string  $\mathcal{X}_M$ . The number of local maxima of the function  $f(\mathcal{X})$  is zero at  $K = 0$  landscape. At  $K > 0$  the number of local maxima increases. Therefore, at  $K = 0$ , the difference  $f(\mathcal{X}_M) - f(\mathcal{X})$  is proportional to the Hamming distance  $d_H(\mathcal{X}_M, \mathcal{X})$  between the vectors [35]. The Hamming distance gives the number of different bits between the two vectors. For example, consider  $\mathcal{X}_1 = (010101)$  and  $\mathcal{X}_2 = (000101)$ . The hamming distance is  $d_H(\mathcal{X}_1, \mathcal{X}_2) = 1$ . At  $K > 0$ , the landscape becomes more complicated because the function  $f$  has additional local maxima beside the global one. Thus the difference  $f(\mathcal{X}_M) - f(\mathcal{X})$  is no longer proportional to the hamming distance  $d_H$ . The average number of local maxima increases with  $K$  until the limiting case of  $K = N - 1$ , in which the landscape becomes completely random, known as the Random Energy model [36].

## 2.2 Computational cost

The time evolution of the system is measured in Monte Carlo steps (MCS). The evolution gets to a halt when one agent reaches the maximum fitness  $F$  of the landscape. Each agent changes its fitness  $f(\mathcal{X})$  when its string  $\mathcal{X}$  is updated (described in next section). So, all agents try to increase their fitness during the time evolution. The dynamics begins at  $t = 0$  with the selection of one agent for a string update. One Monte Carlo step (MCS) is the update of  $M$  random agents, in sequence.

The efficiency of the search is measured by the time  $t_g$  in MCS required by the first agent to find the global maximum  $F$ , in other words, when its string becomes  $\mathcal{X}_M$  after a number of updates. A small  $t_g$  means more efficient search: the goal was achieved in less time. So, the lower the better. The normalized computational cost is then defined as [11]:

$$C \equiv Mt_g/2^N. \quad (3)$$

This normalization ensures  $C$  can be compared between systems of different sizes  $M$  and landscapes  $N$ .

It is important to compare this computational cost with the one from the system considering  $M$  independent agents. This means that each agent does not interact with any other. In this case, the agents are placed on the nodes of a completely disconnected network, containing  $M$  components. This case is used as a reference and has an analytic result [37]:

$$\langle C_I \rangle = \frac{M}{2^N \left[ 1 - (\lambda_N)^M \right]}, \quad (4)$$

where  $\lambda_N$  depends on the value of  $N$ .  $C > C_I$  means the interaction between the agents creates more problems than solution, slowing down the quest of the agents for the global maximum. Otherwise, if  $C < C_I$ , the interaction helped the agents making one of them find the global maximum in less time.

## 2.3 Strings update

Each agent has its string  $\mathcal{X}$  updated when it is selected for analysis. This is how each agent tries to improve its fitness  $f(\mathcal{X})$ , to eventually reaches the global maximum. We call this agent the target, and he can implement one of the two strategies to perform the update: exploitation or exploration [33]. Exploitation implies the target tries to learn the solution from a neighbour with a higher fitness. This is implemented as a copy, with probability  $p$ : the target copies one bit of the string of the model agent [35]. Otherwise, exploration means the target aims to innovate a new solution with a better fitness by itself. It is a mutation on the string of the target, and it should happen with probability  $1 - p$ . However if the target has no neighbors or if it is the model of its influence neighborhood, the mutation will happen for sure. If it has no neighbors, it does not have anyone to copy. And if it is already the model, there is no point in copy another agent with a smaller (worst) fitness. The model agent is the one with the highest fitness in the target influence neighborhood. The target agent may be the model if it has a larger fitness than his neighbors.

Both processes change the string of the target agent. The mutation is achieved by a flip of a random bit of the string. The copy process involves more steps: the different bits between the target and the model strings are selected. Then, one of them is randomly selected and flipped on the target string. This is the imperfect copy on the imitation learning context [31]. As a result, the target string gets more similar to the model string (hamming distance decreases). If  $K = 0$ , this means the target agent increases his fitness. On the other hand, if  $K > 0$ , the model one may be a local maxima, and the hamming distance between the target string  $\mathcal{X}$  and the global maximum one  $\mathcal{X}_M$  may increase when the target copies the local maximum (model agent). The target can get trapped on the suboptimal solution (local maximum) [18].  $K = 0$  is the easy landscape and increasing  $K$  increases the difficulty of the landscape. The most difficult landscape is  $K = N - 1$  where there is no point on copy because the landscape is completely random.

## 2.4 Coevolution mechanism

The general idea of coevolution is to apply a rewiring before each string update: removing a random neighbor and adding a new one to the target agent. However, we can let the number of destroyed and created connections be greater than one. Therefore, before each string update we remove  $L < k_i$  random neighbors and add  $L$  new random neighbors to the target agent. The parameter  $L$  is an input to our model, it is the control parameter of the coevolution process. The static network scenario is recovered with  $L = 0$ .

The rewiring itself is the temporal evolution of the network. To be considered as coevolution, this network evolution must be coupled to the evolution of the agent string. The constant rewiring (always happening) is not coevolution, although it is a network evolution [35]. As the rewiring itself is a random process, the coupling of the network evolution with the agent states, in our model, will be achieved by the probability of rewiring  $r$ : it must be calculated considering

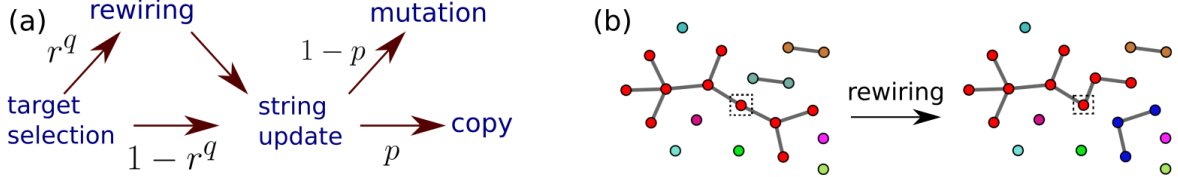


Figure 1: Schematic illustration of the implemented model. (a) Illustration of one iteration. It starts with the selection of the target agent.  $r$  is calculated through Eq. 6. With probability  $r^q$  the network can suffer a rewiring. The next step is the string update, where a copy happens with probability  $p$  and a mutation with probability  $1 - p$ . (b) Illustration of the rewiring process. The target agent (indicated by a dashed black square) loses  $L$  neighbors and gets new  $L$  ones. The case  $L = 1$  is illustrated in this picture: the target loses the neighbor on the right and gets acquainted with the agent right above him. The colors of the nodes indicate the components.

the fitness of the agents. The rewiring process happens before the string update, as illustrated on Fig. 1(a). Another illustration of one example of the rewiring itself (with  $L = 1$ ) is shown Fig. 1(b).

## 2.5 Rewiring probability

The goal of each agent is to increase its fitness until one of them, eventually, reaches the global maximum of the landscape. So, having neighbors with better fitness is beneficial. The probability  $r$  should be larger when most of the neighbors have smaller fitness, so one of them may be replaced with a higher fitness one. The limit cases of this hypothesis are:

- the agent is the model: all neighbors have smaller fitness, so it is justifiable to replace some of them. The probability should be maximum:  $r = 1$ .
- the agent has the smallest fitness of the neighborhood: any copy is already rewarding, so there is no urgency to replace any neighbor. The probability should be minimum:  $r = 0$ .
- Otherwise, the probability should be such as  $0 < r < 1$ .

This behavior is accomplished by the definition:

$$r = \frac{\phi_t - \phi_s}{\phi_m - \phi_s}, \quad (5)$$

where  $\phi_t$  is the fitness of the target agent,  $\phi_s$  is the smallest fitness and  $\phi_m$  is the maximum one (fitness of the model) on the influence neighborhood. Notwithstanding, after extensive tests, we did not find any gain on the computational cost with coevolution using this probability.

We have tested several other definitions for the probability, surprisingly, only one gave interesting results:

$$r = 1 - \frac{\phi_t - \phi_s}{\phi_m - \phi_s}. \quad (6)$$

This is the opposite of the first attempt:  $r = 0$  if the target is the model and 1 if it has the smallest fitness. The assumption from Eq. 5 is based on the update via copy. It is worth mention that this copy happens with probability  $p$ , been the other update process the mutation. So, regardless Eq. 5 seems more plausible, it is possible that other mechanisms (such as Eq. 6) may yield better results. After all, the outcome after a mutation is independent if there was a rewiring or not.

For completeness sake, we add one more parameter to the probability, giving it the form  $r^q$ . The free parameter  $q \geq 0$  controls the frequency of the rewiring:  $q = 1$  (probability is just  $r$ ) enables the coevolution and  $q = 0$  (probability equals 1) implies a constant rewiring. Possible non-linear effects can be examined using other values subjected to the constraint  $q \neq 0$  and  $q \neq 1$  [38].

## 2.6 Random Network

A network or a graph comprises a collection of vertices interconnected by a set of edges [39, 40]. Each edge, or connection, links a pair of vertices with the number of vertices defining the network size and the set of edges determining its connectivity. Vertices that share an edge are termed neighbors. Throughout this work the terms vertices, agents,

and individuals have the same meaning. Various types of networks are used for solutions of physical and biological problems [41, 42, 43]. In this work we will use the Erdős-Rényi (ER) network [44, 45] which has the following definition: consider a set of  $M$  vertices and a parameter  $\beta$  such that  $0 < \beta < 1$ , the probability of any two vertices being connected is  $\beta$ . This network has been used frequently as a first prototype to study the influence of the network topology on social dynamics [46, 47, 48].

The degree  $k_i$  is the number of neighbors of node  $i$  and the average degree  $\mu$  of the network is defined as  $\mu = (1/M) \sum_i^M k_i$  [49]. In the case of ER network, we have  $\mu = \beta(M - 1)$  [4]. So we use  $\mu$  as control parameter of the network instead of  $\beta$ .

### 3 Results

A schematic illustration for our dynamic is presented in Figure 1. The input parameters are  $M, L, p, N, K$  and  $S$ . The general algorithm is:

1. A sample of the random network is created and the time starts at  $t = 0$ .
2.  $t_g$  Monte Carlo Steps are executed until one agent finds the landscape maximum  $F$ . The computational cost is calculated (Eq. 3).
3. Steps 1 and 2 constitute one time evolution.  $S$  random time evolutions are performed and the average  $\langle C \rangle$  computational cost is recorded.

One Monte Carlo step is the execution of  $M$  iterations. The algorithm for one iteration is:

- One random node is selected to serve as the target agent.
- The rewiring happens with probability of  $r^q$  where  $L$  links are removed and new  $L$  links are created involving the target agent.
- The string update takes place and it can be either a mutation or a copy.

Fig. 1(a) illustrates this algorithm and 1(b) shows an example of the rewiring with  $L = 1$ .

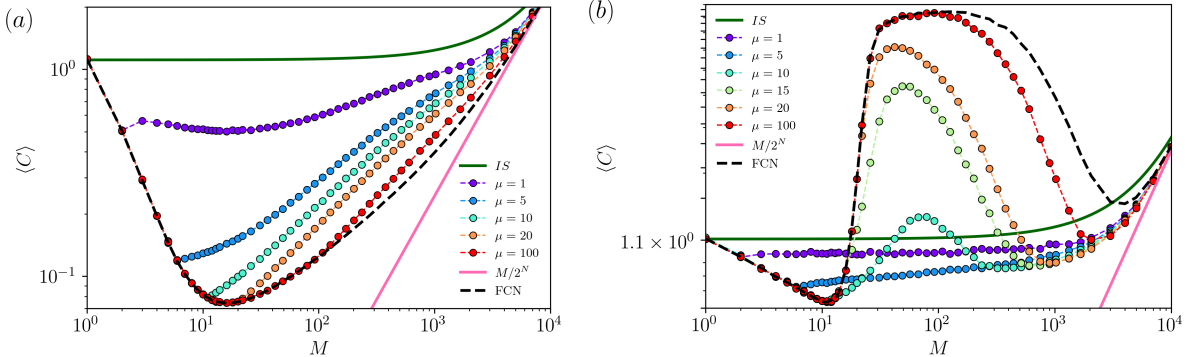


Figure 2: Results of the Reference Case on the two investigated landscapes. Computational cost  $\langle C \rangle$  as function of  $M$  for different average degrees  $\mu$  of the ERN with no coevolution. These results is the reference to which we will compare the results with coevolution to evaluate its impact. Parameter:  $q = 1$  and  $S = 5 \times 10^4$  samples. The green line is the IS (Eq. 4), black dashed line is the FCN result and the pink line is the approximation for large  $M$ . Purple, blue, green, orange and red circles correspond to an average degree of  $\mu = 1, 5, 10, 20$  and  $100$ , respectively. (a) Easy landscape:  $K = 0$ . (b) Difficult landscape:  $K = 4$ .

In this work we explored two values for the  $K$  parameter:  $K = 0$  is the easy case and  $K = 4$  is the complicated one. We also investigated the following values for the coevolution:  $L = 0, 1, 2, 3, 4, 5$  and  $6$ . We also fixed  $N = 12$  and the copy probability at  $p = 0.5$ . At this value of  $N$  we have  $\lambda_{12} \approx 0.99978$ . Since  $(\lambda_{12})^M \approx e^{-M(1-\lambda_{12})}$ , we can approximate the limit cases (low and large  $M$ ) of the independent search from Eq. 4 as [28, 37]:

$$\langle C_I \rangle \approx \begin{cases} 1.110, & \text{for } M \ll 4545 \\ M/2^{12}, & \text{for } M \gg 4545 \end{cases} \quad (7)$$

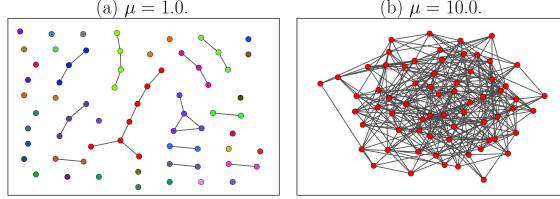


Figure 3: Snapshots of instances of the random network used in this work. System size:  $M = 67$  agents. Each component is represented in a different color. (a) Low average degree scenario:  $\mu = 1.0$ . The network is not percolated and the largest component is in painted in red. (b) High average degree scenario:  $\mu = 10.0$ . In this scenario the network is percolated.

### 3.1 Benchmark

In order to better assess the impact of the coevolution porcess, we compare its results to 3 others data sets:

- Independent Search (IS): when each agent independently searches for the global maximum. In this case there is no copy of the model strings, only mutation. Numerically, it can be achieved by setting  $p = 0$  or using a network with  $k_i = 0$  for all agents  $i$ . Analytically, it can be calculated using Eq. 4, and its limit cases for small and large  $M$  are given by Eq. 7. This result will be displayed as a green solid line on the results.
- Full Connected Network (FCN): when all agents are connected to all other agents:  $k_i = M - 1$  for all agents. This result will be displayed as a black dashed line on the results.
- Reference Case (RC): dynamics with a static network, no rewiring, equivalent to  $L = 0$ . Coevolution will bring an advantage if it entails a lower computational cost  $C$  than the Reference Case one.

The independent search is the simplest method, and the cheapest one if we think in terms of a company hiring employees to perform the task. The FCN case is also a simple one, however not the cheapest one. As  $M$  increases, the cost to enable everybody to communicate with everybody also increases. Hence, for any particular dynamics to be called efficient, it must bring more efficiency than these two cases.

### 3.2 Reference case

Firstly we present the results with a static network: the Reference Case (RC). It is important to understand this case so we can highlight the effect of the coevolution. At  $K = 0$  (Figure 2(a)) the best result (lower  $\langle C \rangle$ ) is given by the full connected network (FCN) and the worst by the independent search (IS). The increasing average degree  $\mu$  interpolates from IS to the FCN case. As there is only one maximum (the global one) it becomes easier to increase the fitness with more neighbors to copy. However, in terms of system size  $M$  there is one optimal value roughly between 15 and 20 which returns  $\langle C \rangle \sim 0.007$ . So, if there is too few neighbors (smaller  $M$ ) or too much neighbors (larger  $M$ ) the agents spend more time looking for the global maximum. At large  $M \gtrsim 10^4$  the system behaviors as the limit case  $M/2^N$ .

When  $K = 4$  (Figure 2(b)) the scenario is drastically different. As before there is an optimal value of  $M$  roughly between 10 and 15. However there is a significant increase on the cost  $\langle C \rangle$  at  $M \gtrsim 20$  when  $\mu$  is increased towards the FCN. As there are local maxima in this landscape, an agent can be trapped in one of these making it longer to find the global maxima. The results on these two scenarios resemble the similar case on the random geometric graph [35].

### 3.3 Dynamics with coevolution

To enhance the effect of coevolution, we restricted the values of the average degree for the analysis. We observed different scenarios for different values of this degree: coevolution works for some cases and does not work at other cases. We say it works when the computational cost  $\langle C \rangle$  is lower compared to the Reference Case, keeping all other parameters the same. We found local improvements on  $\langle C \rangle$  at the degrees  $\mu = 1.0$  and  $\mu = 10.0$  (see Fig. 3). These are the scenarios where coevolution works (at some values of  $M$ ), depicted in Figs. 4, 5 and 8(a). The scenarios where it does not work are depicted in Figs. 8(b) and 8(c).

Let's start with the low average degree scenario, Fig. 3(a). Considering the easy landscape with  $K = 0$  (Fig. 4(a)), the coevolution brings benefit to the cost except when  $L = 1$ . As there is only one maximum, any other agent with a higher fitness is worth copying. And this process is facilitated by the selective rewiring of the coevolution. Interestingly, the

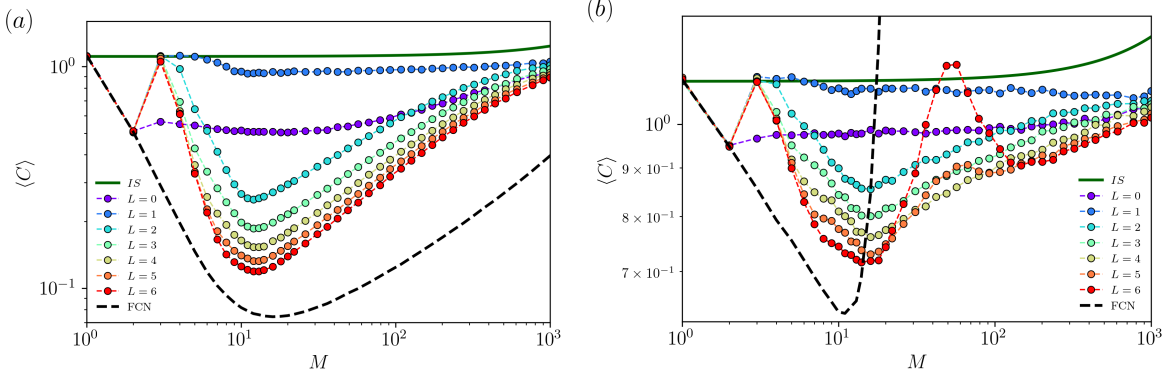


Figure 4: Coevolution results in a low degree network ( $\mu = 1$ ) on the two investigated landscapes. Computational cost  $\langle C \rangle$  vs.  $M$  for different values of modification  $L$ , limited by  $L < k_i$  for each agent.  $L = 0$  means no coevolution. Parameters:  $S = 10^5$  samples and  $\mu = 1$ . The green line is the IS (Eq. 4) and the black dashed line is the FCN result. (a) Easy landscape:  $K = 0$ . (b) Difficult landscape:  $K = 4$ .

case  $L = 1$  increases the cost. The difficult case  $K = 4$  (Fig. 4(b)) has some similarities: the cost increases at  $L = 1$  and then decreases up to  $L = 5$ . At  $L = 6$  there is a significant increase only at  $M \sim 60$ .

At higher average degree (Fig. 3(b)) the results are drastically different. The ease case  $K = 0$  (Fig. 5(a)) shows influence of  $L$  only on small network sizes around  $M \lesssim 15$ . At  $K = 4$  the results become more interesting. At small networks, coevolution continues to present a higher computational cost. However, at medium-sized networks ( $20 \leq M \leq 120$ ), we see a significant improvement in computational cost:  $\langle C \rangle$  presents a maximum at  $M = 67$  for  $L = 0$  (Fig. 5(b)) and a minimum at  $L = 3$ .

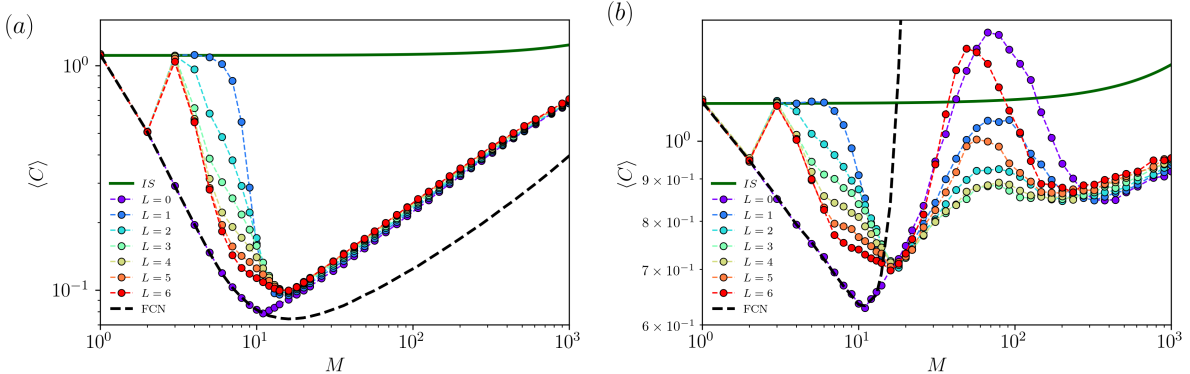


Figure 5: Coevolution results in a high degree network ( $\mu = 10$ ) on the two investigated landscapes. Computational cost  $\langle C \rangle$  vs.  $M$  for different values of modification  $L$ , limited by  $L < k_i$  for each agent.  $L = 0$  means no coevolution. Parameters:  $S = 10^5$  and  $\mu = 10$ . The green line is the IS (Eq. 4) and the black dashed line is the FCN result. (a) Easy landscape:  $K = 0$ . (b) Difficult landscape:  $K = 4$ .

The minimum of  $\langle C \rangle$  with respect to  $L$  has a larger sensitivity to  $M$  than with to  $\mu$ . As can be seen on Fig. 6(a), the cost has a pronounced minimum between  $L = 2$  and 3 considering different values of  $M$ . However, when  $M$  is fixed and  $\mu$  is varied, the minimum is not so evident (Fig. 6(b)), and even not present at some values.

To better visualize the behavior of the  $\langle C \rangle$  minimum at  $M = 67$ , Fig. 7(a) displays a color map on the space  $(L, \mu)$ . However, a more interesting measure is the difference between the  $L = 3$  and  $L = 0$  values, defined as:

$$\Delta(L, \mu) = \langle C \rangle(L, \mu) - \langle C \rangle(0, \mu). \quad (8)$$

This quantity gives the improvement ( $\Delta < 0$ ) on the cost  $\langle C \rangle$  created by the coevolution, as can be seen on Fig. 7(b). The average degree has a great impact on this gain: at  $L = 6$  it goes from destroying it at  $\mu = 6$  to improving the performance at  $\mu = 12$ . This result shows the tunable coevolution described here is a real tool to increase performance on the NK model.

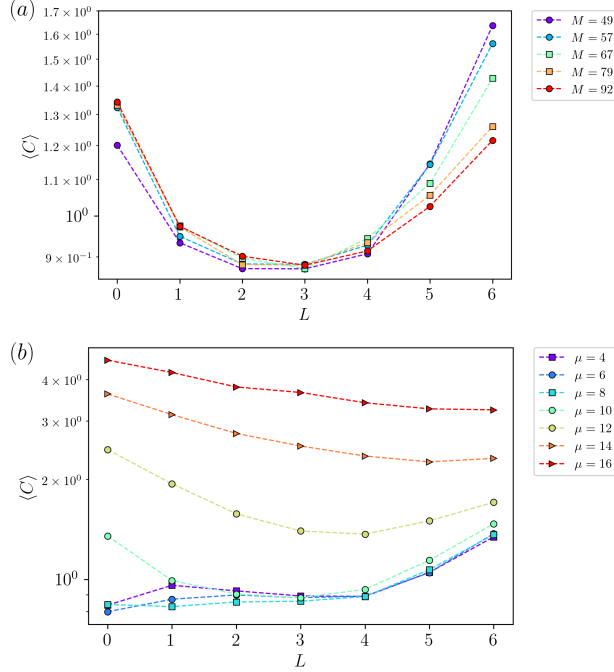


Figure 6: Characterization of the computational cost minimum caused by the coevolution. Computational cost  $\langle C \rangle$  vs.  $L$ . Parameters:  $K = 4$ ,  $q = 0$  and  $S = 30000$ . (a) Minimum on the  $(M, L)$  space. Different values of  $M$  while  $\mu = 10$ . (b) Different values of  $\mu$  while  $M = 67$ .

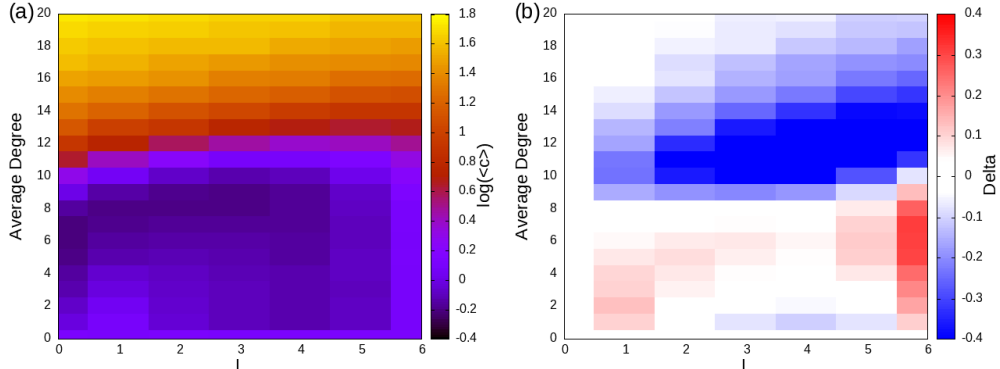


Figure 7: 2D map of the computational cost  $\langle C \rangle$  and its gain  $\Delta$  in the  $(L, \mu)$  space. Parameters:  $K = 4$ ,  $q = 1$ ,  $M = 67$  and  $S = 10^5$ . (a)  $\log(\langle C \rangle)$ . (b)  $\Delta$  defined on Eq. 8. Positive values are indicated in red and negative values in blue.

### 3.4 Other dynamics

We now verify the differences between the coevolution ( $q = 1$ ) and constant rewiring ( $q = 0$ ) dynamics. Considering the curve  $L = 1$  from Fig. 5(b), the constant rewiring case gives a lower cost, as can be seen on Fig. 8(a). Focusing on the peak at  $M \sim 67$ , the results show a slightly better performance (lower cost) with  $L = 1$  for the constant rewiring case, while negligible differences when  $L = 3$ . Figures 8(b) and 8(c) show these same results for different average degrees  $\mu$ , where coevolution itself does not work. One can see on these results that constant rewiring does not work either.

Lastly we studied the impact of non-linearity on the computational cost, which happens when  $q$  is different from 0 or 1 [38]. In this work non-linearity yield no significant outcome, as can be shown on Fig. 9. The case  $q = 0.5$  only showed slightly better performance than the linear case  $q = 1$  around  $M = 67$ . Other than this region there were no significant differences.

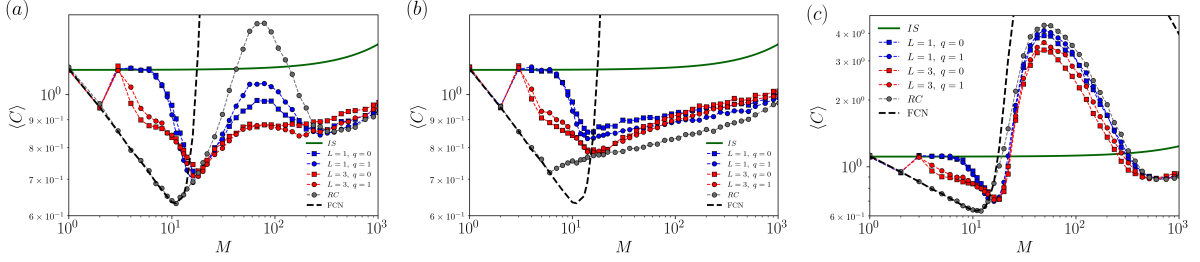


Figure 8: Comparison between coevolution and constant rewiring dynamics. Computational cost  $\langle C \rangle$  as a function of network size  $M$  for different values of the average degree. The green line is the IS (Eq. 4), the black dashed line is the FCN result and RC is the reference case (equivalent to  $L = 0$ ). (a) Scenario where coevolution works: average degree  $\mu = 10$ . Scenarios where coevolution does not work: (b)  $\mu = 5$  and (c)  $\mu = 15$ .

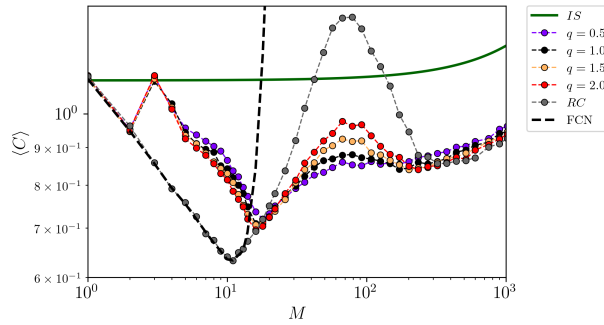


Figure 9: Study of the impact of non-linear effects on the coevolution dynamics. Computational cost  $\langle C \rangle$  vs.  $M$  for different values of the non-linear parameter  $q$ . Parameters:  $\mu = 10$ ,  $S = 3000$  and  $L = 3$ . The violet circles correspond to  $q = 0.5$ , the orange circles to  $q = 1.5$ , and the red circles to  $q = 2.0$ . The reference case RC ( $L = 0$  and  $q = 1$ ) is depicted in gray. The non-linear case refers to  $q \neq 0$  and  $q \neq 1.0$ .

## 4 Conclusions

We investigated the impact of coevolution on a cooperative process, where the target can substitute a few of his neighbors in order to solve the problem more rapidly. The neighbors are important because copy one of them (exploitation) is one possible strategy to improve the fitness. So, each agent analyses the fitness of his neighbors and uses this piece of information to decide whether or not to substitute a few of them. The number of neighbors to be replaced is an input parameter of the model. This creates a tunable mechanism enabling some sort of intensity on the coevolution process: a “weak” coevolution would be  $L = 1$ , which has been studied on different social models. A “stronger” coevolution would be  $L \geq 2$ , which, to the best of our knowledge, has not been studied before.

A natural strategy for the target is to change some of his neighbors if they have worst (smaller) fitness than him. Nonetheless, this rule did not give satisfactory results in our tests when compared with the reference case. Surprisingly, the opposite rule did yield some interesting results. We chose to apply this new coevolution model on a cooperative process. Using as prototype the NK model, our results showed a convoluted behavior of the system efficiency.

At the easy landscape, coevolution did bring significantly better results only at lower average degree (Fig. 4(a)). Additionally, the larger  $L$  the lower the  $C$ , except at  $L = 1$  at which the results are worse. However, the FCN case is still the more efficient one at  $K = 0$ , regardless other parameters. At the difficult landscape  $K = 4$ , the behaviour was unanticipated. At lower average degree, after a cost increase at  $L = 1$ , the cost cutback for increasing  $L$  for most part of the system size range. Except at around  $M \sim 70$  where a peak starts to grow at  $L = 5$  and becomes higher than the IS cost (Fig. 4(b)). At higher average degree, this peak on the cost already exists at  $L = 0$  (Fig. 5(b)). It disappears at  $L = 3$  and comes back at  $L = 5$ . Indeed, this minimum can be better visualized on the  $(M, L)$  space (Fig. 6(a)). Fixing  $M = 67$ , the minimum of the computational cost can be seen in details on the 2D map of Fig. 7(b) (blue region).

This work showed that this tunable coevolution can drastically change the behavior of computational cost. It opens some interesting perspectives such as the impact of this tunable coevolution on the phase diagram involving absorbing phase transition of models such as Axelrod's, voter model and others.

## Acknowledgements

This work received financial support from the brazillian agencies CNPq (project 405508/2021-2) and FAPEG (project no. 401425/2023-1). This research was also supported by LaMCAD/UFG.

## Author contributions

**Francis F. Franco:** Conceptualization, Methodology, Software, Formal analysis, Investigation, Writing - Original Draft, Writing - Review e Editing, **Paulo F. Gomes:** Conceptualization, Methodology, Formal analysis, Investigation, Writing - Original Draft, Writing - Review, Editing, Supervision, Project administration. Authors declare that there are no competing interests.

## Data Availability Statement

The model was implemented using Fortran and the analysis and graphics were developed using Python (packages: Numpy [50], Matplotlib [51], NetworkX [52] and Pandas [53]) and Gnuplot.

## A Appendix

### A.1 NK landscape

In this appendix we present a simplified description of how the function  $f(\mathcal{X})$  is created for a given landscape.

Following the formal definition from Eq. 1, we have  $f : \mathcal{D} \rightarrow \mathcal{R}$ , where  $\mathcal{D}$  is the set of  $2^N$  binary vectors  $\mathcal{X}$  and  $\mathcal{R}$  is the real numbers set. The argument of the contributing functions  $\Phi_i$  is given by Eq. 2. To better understand this, suppose the vector  $\mathcal{Y} = (y_0, y_1, y_2, y_3) = (0, 1, 1, 0)$  on the landscape  $N = 4$  and  $K = 2$ . There will be  $K + 1 = 3$  bits on the argument of each  $\Phi_i$ . The first bit from the  $i$ -th contribution is the  $i$ -th bit of  $\mathcal{Y}$ , while the other bits are the  $K = 2$  neighbors on the right. So, the first contribution of  $\mathcal{Y}$  is  $\Phi_0(y_0, y_1, y_2) = (0, 1, 1)$ . The second contribution will be  $\Phi_1(y_1, y_2, y_3) = \Phi_1(1, 1, 0)$ . On the third contribution  $\Phi_2$ , the third bit will be the fifth one of  $\mathcal{Y}$ . However, and the string  $\mathcal{Y}$  has only  $N = 4$  bits, so the fifth bit will be the first one. This is equivalent to subtract  $N$  from the position of the bit:  $5-4 = 1$ . Thus:  $\Phi_2(y_2, y_3, y_0) = \Phi_2(1, 0, 0)$ . In the same way:  $\Phi_3(y_3, y_0, y_1) = \Phi_3(0, 0, 1)$ . Putting together the four contributions, we have:

$$\begin{aligned} f(0, 1, 1, 0) &= \frac{1}{4}\Phi_0(0, 1, 1) + \frac{1}{4}\Phi_1(1, 1, 0) \\ &+ \frac{1}{4}\Phi_2(1, 0, 0) + \frac{1}{4}\Phi_3(0, 0, 1). \end{aligned} \quad (9)$$

Other examples are:

$$\begin{aligned} f(0, 0, 0, 0) &= \frac{1}{4}\Phi_0(0, 0, 0) + \frac{1}{4}\Phi_1(0, 0, 0) \\ &+ \frac{1}{4}\Phi_2(0, 0, 0) + \frac{1}{4}\Phi_3(0, 0, 0), \\ f(0, 0, 1, 0) &= \frac{1}{4}\Phi_0(0, 0, 1) + \frac{1}{4}\Phi_1(0, 1, 0) \\ &+ \frac{1}{4}\Phi_2(1, 0, 0) + \frac{1}{4}\Phi_3(0, 0, 0), \\ f(1, 0, 1, 0) &= \frac{1}{4}\Phi_0(1, 0, 1) + \frac{1}{4}\Phi_1(0, 1, 0) \\ &+ \frac{1}{4}\Phi_2(1, 0, 1) + \frac{1}{4}\Phi_3(0, 1, 0), \\ f(0, 1, 1, 1) &= \frac{1}{4}\Phi_0(0, 1, 1) + \frac{1}{4}\Phi_1(1, 1, 1) \\ &+ \frac{1}{4}\Phi_2(1, 1, 0) + \frac{1}{4}\Phi_3(1, 0, 1), \\ f(1, 1, 1, 1) &= \frac{1}{4}\Phi_0(1, 1, 1) + \frac{1}{4}\Phi_1(1, 1, 1) \\ &+ \frac{1}{4}\Phi_2(1, 1, 1) + \frac{1}{4}\Phi_3(1, 1, 1). \end{aligned}$$

It is worth mention that each argument on the functions  $\Phi_i$  contains  $K + 1$  bits. So, there are  $2^{K+1}$  possible combinations for the  $N$  contributions from each vector.

## A.2 Base 2 and 10

Conceptually, the description from previous section is enough. However, computationally, it is compelling to represent the vectors  $\mathcal{X}$  and the arguments of the contributions  $\Phi_i$  as integers. Both of them are binary sequences, 0s and 1s, numbers in base 2, and thus, can be converted to decimal numbers (base 10). In general, considering  $N = 4$ :  $(x_0, x_1, x_2, x_3) = x_3 \cdot 2^0 + x_2 \cdot 2^1 + x_1 \cdot 2^2 + x_0 \cdot 2^3$ , starting the count from the right. Thus,

$$\begin{aligned} (0, 0, 0, 0) &= 0, & (0, 0, 0, 1) &= 1, \\ (0, 0, 1, 0) &= 2, & (0, 1, 0, 0) &= 4, \\ (1, 0, 0, 0) &= 8, & (0, 1, 0, 1) &= 5. \end{aligned}$$

Computationally, this is much more efficient because we can record each string by its base 10 correspondent number (an integer), which takes much less memory than the string with  $N$  bits.

We can do the same for the arguments of the contribution functions. Eq. 9 would be:

$$\begin{aligned} f(0, 1, 1, 0) &= f(6), \\ &= \frac{1}{4} [\Phi_0(3) + \Phi_1(6) + \Phi_2(4) + \Phi_3(1)]. \end{aligned}$$

Other example: the fitness of the vector  $\mathcal{X} = 7$  considering  $N = 4$  and  $K = 3$  is:

$$\begin{aligned} f(7) &= f(0, 1, 1, 1), \\ &= \frac{1}{4} \Phi_0(0, 1, 1) + \frac{1}{4} \Phi_1(1, 1, 1) \\ &+ \frac{1}{4} \Phi_2(1, 1, 0) + \frac{1}{4} \Phi_3(1, 0, 1), \\ &= \frac{1}{4} [\Phi_0(3) + \Phi_1(7) + \Phi_2(6) + \Phi_3(5)]. \end{aligned}$$

This binary to decimal conversion is performed only once, when the landscaped is built, in the beginning of the algorithm. The fitness is the function  $f(i)$  where  $i = 0, 1, 2, 3, \dots, 2^N - 1$ . Likewise, the contributions are functions  $\Phi_i(j)$  where  $i = 0, 1, 2, 3, \dots, N - 1$  and  $j = 0, 1, 2, 3, \dots, 2^{K+1} - 1$ . Initially, the vectors  $\mathcal{X}$  are randomly generated, which can be done by generating random integers from 0 to  $2^N - 1$  using a uniform distribution.

Once the arguments are defined, we have to define the functions  $\Phi_i(j)$  itself. In this work, we use the NK landscape for a cooperative problem where the simulation comes to a halt when one agent finds the global maximum. So, it is interesting to keep the fitness on the range  $[0, 1]$ . Thus, we define the functions  $\Phi_i(j)$  as a random number from the uniform distribution on the same range  $[0, 1]$ .

## References

- [1] C. Castellano, S. Fortunato, V. Loreto, Statistical physics of social dynamics. *Review of Modern Physics* **81**, 591 (2009). <https://doi.org/10.1103/RevModPhys.81.591>.
- [2] M. Perc, A. Szolnoki, Coevolutionary games - A mini review. *BioSystems* **99**, 109-125 (2010). <https://doi.org/10.1016/j.biosystems.2009.10.003>.
- [3] M. Jusup, P. Holme, K. Kanazawa, M. Takayasu, I. Romic, Z. Wang, S. Gecek, T. Lipic, B. Podobnik, L. Wang, W. Luo, T. Klanjšček, J. Fan, S. Boccaletti, M. Perc, Social Physics. *Physics Reports* **948**, 1-148 (2022). <https://doi.org/10.1016/j.physrep.2021.10.005>.
- [4] A. L. Barabási, *Network Science*, Cambridge University Press, Glasgow (2016). <https://networksciencebook.com/>.
- [5] T. Gross, B. Blasius, Adaptive coevolutionary networks: a review. *Journal of the Royal Society Interface* **5**, 259-271 (2008). <https://doi.org/10.1098/rsif.2007.1229>.
- [6] V. Marceau, P.-A. Noël, L. Hébert-Dufresne, A. Allard, L. J. Dubé, Adaptive networks: Coevolution of disease and topology. *Physical Review E* **82**, 036116 (2010). <https://link.aps.org/doi/10.1103/PhysRevE.82.036116>.
- [7] J. Choi, B. Min, Coevolutionary Dynamics of Information Spreading and Heterophilic Link Rewiring. *New Physics: Sae Mulli* **73**, 886-892 (2023). <https://doi.org/10.3938/NPSM.73.886>.
- [8] M. G. Zimmermann, V. M. Eguíluz, Cooperation, social networks, and the emergence of leadership in a prisoner's dilemma with adaptive local interactions. *Physical Review E* **72**, 056118 (2005). <https://doi.org/10.1103/PhysRevE.72.056118>.

[9] Z. Qin, Z. Hu, X. Zhou, J. Yi, Age structure and cooperation in coevolutionary games on dynamic network. *European Physical Journal B* **88**, 92 (2015). <https://doi.org/10.1140/epjb/e2015-50680-x>.

[10] T. Raducha, M. Wiliński, T. Gubiec, H. E. Stanley, Statistical mechanics of a coevolving spin system. *Physical Review E* **98**, 030301 (2018). <https://doi.org/10.1103/PhysRevE.98.030301>.

[11] S. M. Reia, P. F. Gomes, J. F. Fontanari, Policies for allocation of information in task-oriented groups: elitism and egalitarianism outperform welfarism. *The European Physical Journal B* **92**, 205 (2019). <https://doi.org/10.1140/epjb/e2019-100345-7>.

[12] M. Saeedian, M. S. Miguel, R. Toral, Absorbing-state transition in a coevolution model with node and link states in an adaptive network: network fragmentation transition at criticality. *New Journal of Physics* **22**, 113001 (2020). <https://doi.org/10.1088/1367-2630/abbfd0>.

[13] S. M. Reia, P. F. Gomes, J. F. Fontanari, Comfort-driven mobility produces spatial fragmentation in Axelrod's model. *Journal of Statistical Mechanics* 033402 (2020). <https://doi.org/10.1088/1742-5468/ab75e5>.

[14] P. F. Gomes, H. A. Fernandes, A. A. Costa, Topological transition in a coupled dynamics in random networks. *Physica A: Statistical Mechanics and its Applications* **597**, 127269 (2022). <https://doi.org/10.1016/j.physa.2022.127269>.

[15] A. Szolnoki, M. Perc, Coevolution of teaching activity promotes cooperation. *New Journal of Physics* **10**, 043036 (2008). <http://dx.doi.org/10.1088/1367-2630/10/4/043036>.

[16] A. Szolnoki, and M. Perc, Promoting cooperation in social dilemmas via simple coevolutionary rules. *European Physical Journal B* **67**, 337-344 (2009). <http://dx.doi.org/10.1140/epjb/e2008-00470-8>.

[17] N. R. F. Maier, L. R. Hoffman, Quality of first and second solutions in group problem solving. *Journal of Applied Psychology* **44**, 278-283 (1960). <https://doi.org/10.1037/h0041372>.

[18] D. Lazer, A. Friedman, The Network Structure of Exploration and Exploitation. *Administrative Science Quarterly* **52**, 667-694 (2007). <https://doi.org/10.2189/asqu.52.4.667>.

[19] S. M. Reia, P. F. Gomes, J. F. Fontanari, Individual decision making in task-oriented groups. *European Physical Journal B* **92**, 109 (2019). <https://doi.org/10.1140/epjb/e2019-90732-7>.

[20] L. Rendell, R. Boyd, D. Cownden, M. Enquist, K. Eriksson, M. W. Feldman, L. Fogarty, S. Ghirlanda, T. Lillicrap, K. N. Laland, Why Copy Others? Insights from the Social Learning Strategies Tournament. *Science* **328**, 208-213 (2010). <https://doi.org/10.1126/science.118471>.

[21] M. Zare , P. M. Kebria, A. Khosravi, S. Nahavandi, A Survey of Imitation Learning: Algorithms, Recent Developments, and Challenges. *IEEE Transactions on Cybernetics* 1-14 (2024). <https://doi.org/10.1109/TCYB.2024.3395626>.

[22] J. F. Fontanari, Imitative Learning as a Connector of Collective Brains. *PLoS ONE* **9**, e110517 (2014). <http://dx.doi.org/10.1371/journal.pone.0110517>.

[23] V. Capraro, M. Perc, In search of the most cooperative network. *Nature Computational Science* **4**, 257-258 (2024). <https://doi.org/10.1038/s43588-024-00623-6>.

[24] S. A. Kauffman, S. Levin, Towards a general theory of adaptive walks on rugged landscapes. *Journal of Theoretical Biology* **128**, 11-45 (1987). [https://doi.org/10.1016/S0022-5193\(87\)80029-2](https://doi.org/10.1016/S0022-5193(87)80029-2).

[25] S. A. Kauffman, Adaptation on rugged fitness landscapes. In: *Complex Systems, SFI Studies in the Sciences of Complexity* (Stein, D., ed.) New York: Addison-Wesley Longman, (1989).

[26] S. A. Kauffman, E. D. Weinberger, The N K Model of Rugged Fitness Landscapes And Its Application to Maturation of the Immune Response. *Journal of Theoretical Biology* **141**, 211-245 (1989). [https://doi.org/10.1016/S0022-5193\(89\)80019-0](https://doi.org/10.1016/S0022-5193(89)80019-0).

[27] S. A. Kauffman, *Origins of Order: Self-Organization and Selection in Evolution*. New York: Oxford University Press (1993). <https://doi.org/10.1093/oso/9780195079517.001.0001>.

[28] J. F. Fontanari, F. A. Rodrigues, Influence of network topology on cooperative problem-solving systems. *Theory Bioscience* **135**, 101-110 (2016). <https://doi.org/10.1007/s12064-015-0219-1>.

[29] D. Barkoczi, M. Galesic, Social learning strategies modify the effect of network structure on group performance. *Nature Communications* **7**, 13109 (2016). <https://doi.org/10.1038/ncomms13109>.

[30] M. Ganco, NK model as a representation of innovative search. *Research Policy* **46**, 1783-1800 (2017). <http://dx.doi.org/10.1016/j.respol.2017.08.009>.

[31] G. Yao, J. Wang, B. Cui, Y. Ma, Quantifying effects of tasks on group performance in social learning. *Humanities and Social Sciences Communications* **9**, 282 (2022). <https://doi.org/10.1057/s41599-022-01305-2>.

- [32] J. F. Fontanari, When more of the same is better. *European Physics Letters* **113**, 28009 (2016). <http://dx.doi.org/10.1209/0295-5075/113/28009>.
- [33] F. Baumann, A. Czaplicka, I. Rahwan, Network structure shapes the impact of diversity in collective learning. *Scientific Reports* **14**, 2491 (2024). <https://doi.org/10.1038/s41598-024-52837-3>.
- [34] S. M. Reia, J. F. Fontanari, Effect of group organization on the performance of cooperative processes, *Ecological Complexity* **30**, 47-56 (2017). <http://dx.doi.org/10.1016/j.ecocom.2016.09.002>.
- [35] P. F. Gomes, S. M. Reia, F. A. Rodrigues, J. F. Fontanari, Mobility helps problem-solving systems to avoid groupthink. *Physical Review E* **99**, 032301 (2019). <https://doi.org/10.1103/PhysRevE.99.032301>.
- [36] B. Derrida, Random-energy model: An exactly solvable model of disordered systems. *Physical Review B* **24**, 2613 (1981). <https://doi.org/10.1103/PhysRevB.24.2613>.
- [37] J. F. Fontanari, Exploring NK fitness landscapes using imitative learning. *European Physical Journal B* **88**, 251 (2015). <http://dx.doi.org/10.1140/epjb/e2015-60608-1>.
- [38] T. Raducha, M. S. Miguel, Emergence of complex structures from nonlinear interactions and noise in coevolving networks. *Scientific Reports* **10**, 15660 (2020). <https://doi.org/10.1038/s41598-020-72662-8>.
- [39] M. E. J. Newman, Networks: an introduction. Oxford University Press, Oxford (2010). <https://doi.org/10.1093/oso/9780198805090.001.0001>.
- [40] A. S. da Mata, Complex Networks: a Mini-review. *Brazilian Journal of Physics* **50**, 658-672 (2020). <https://doi.org/10.1007/s13538-020-00772-9>.
- [41] E. B. Vilela, H. A. Fernandes, F. L. P. Costa, P. F. Gomes, Phase diagrams of the Ziff–Gulari–Barshad model on random networks. *Journal of Computational Chemistry* **41**, 1964-1972 (2020). <https://doi.org/10.1002/jcc.26366>.
- [42] A. M. Pineda, P. Kent, C. Connaughton, F. A. Rodrigues, Machine learning-based prediction of Q-voter model in complex networks. *Journal of Statistical Mechanics* 123402 (2023). <https://doi.org/10.1088/1742-5468/ad06a6>.
- [43] Y. L. Silva, A. de A. Costa, Periodic boundary condition effects in small-world networks. *European Physical Journal B* **97**, 105 (2024). <https://doi.org/10.1140/epjb/s10051-024-00746-9>.
- [44] R. Solomonoff, A. Rapoport, Connectivity of random networks. *Bulletin of Mathematical Biology* **13**, 107-117 (1951). [https://doi.org/10.1016/S0092-8240\(76\)80054-7](https://doi.org/10.1016/S0092-8240(76)80054-7).
- [45] P. Erdős, A. Rényi, On random graphs. *Publicationes Mathematicae* **6**, 290-297 (1959).
- [46] P. Holme, M. E. J. Newman, Nonequilibrium phase transition in the coevolution of networks and opinions. *Physical Review E* **74**, 056108 (2006). <https://link.aps.org/doi/10.1103/PhysRevE.74.056108>.
- [47] T. W. Moore, P. D. Finley, B. J. Apelberg, B. K. Ambrose, N. S. Brodsky, T. J. Brown, C. Husten, R. J. Glass, An opinion-driven behavioral dynamics model for addictive behaviors. *European Physical Journal B* **88**, 95 (2015). <https://doi.org/10.1140/epjb/e2015-40462-y>.
- [48] M. Saeedian, M. Miguel, R. Toral, Absorbing phase transition in the coupled dynamics of node and link states in random networks. *Scientific Reports* **9**, 9726 (2019). <https://doi.org/10.1038/s41598-019-45937-y>.
- [49] P. F. Gomes, Uma introdução à Ciência de Redes e Teoria de Grafos, *Revista Brasileira de Ensino de Física* **46**, e20240190 (2024). <https://doi.org/10.1590/1806-9126-RBEF-2024-0190>.
- [50] C. R. Harris, *et al.* Array programming with numpy. *Nature* **585**, 357-362 (2020). <https://doi.org/10.1038/s41586-020-2649-2>.
- [51] J. D. Hunter, Matplotlib: A 2d graphics environment. *Computing in Science & Engineering* **9**, 90-95 (2007). <https://doi.org/10.1109/MCSE.2007.55>.
- [52] A. A. Hagberg, D. A. Schult, P. J. Swart, Exploring network structure, dynamics and function using networkx. *Proceedings of the 7th Python in Science Conference (SciPy2008)* **445**, 11-15 (2008). [http://dx.doi.org/http://conference.scipy.org/proceedings/SciPy2008/paper\\_2/](http://dx.doi.org/http://conference.scipy.org/proceedings/SciPy2008/paper_2/).
- [53] W. McKinney, Data structures for statistical computing in python. *Proceedings of the 9th Python in Science Conference* **445**, 51-56 (2010). <https://doi.org/10.25080/Majora-92bf1922-00a>.